

PCCP

Accepted Manuscript



This is an *Accepted Manuscript*, which has been through the Royal Society of Chemistry peer review process and has been accepted for publication.

Accepted Manuscripts are published online shortly after acceptance, before technical editing, formatting and proof reading. Using this free service, authors can make their results available to the community, in citable form, before we publish the edited article. We will replace this *Accepted Manuscript* with the edited and formatted *Advance Article* as soon as it is available.

You can find more information about *Accepted Manuscripts* in the [Information for Authors](#).

Please note that technical editing may introduce minor changes to the text and/or graphics, which may alter content. The journal's standard [Terms & Conditions](#) and the [Ethical guidelines](#) still apply. In no event shall the Royal Society of Chemistry be held responsible for any errors or omissions in this *Accepted Manuscript* or any consequences arising from the use of any information it contains.

Microscopic interactions of the imidazolium-based ionic liquid with molecular liquids depending on their electron-donicity

Toshiyuki Takamuku^{1,*}, Hiroshi Hoke¹, Abdenacer Idrissi², Bogdan A. Marekha^{2,3}, Myriam Moreau², Yusuke Honda¹, Tatsuya Umecky¹, and Takuya Shimomura⁴

Received (in XXX, XXX) Xth XXXXXXXXXX 20XX, Accepted Xth XXXXXXXXXX 20XX

DOI: 10.1039/b000000x

¹Department of Chemistry and Applied Chemistry, Graduate School of Science and Engineering, Saga University, Honjo-machi, Saga 840-8502, Japan

²Laboratoire de Spectrochimie Infrarouge et Raman (UMR CNRS 8516), University of Lille 1, Nord de France, 59655 Villeneuve d'Ascq Cedex, France

³Department of Inorganic Chemistry, V. N. Karazin Kharkiv National University, 4 Svobody sq., 61022 Kharkiv, Ukraine

⁴Division of Sustainable and Environmental Engineering, Graduate School of Engineering, Muroran Institute of Technology, 27-1 Mizumoto-cho, Muroran, Hokkaido 050-8585, Japan

ABSTRACT

Microscopic interactions of imidazolium-based ionic liquid, 1-ethyl-3-methylimidazolium bis(trifluoromethanesulfonyl)imide ($C_2mimTFSI$), with dimethyl sulfoxide (DMSO), methanol (MeOH), and acetonitrile (AN) have been analyzed by means of Raman, attenuated total reflectance infrared (ATR-IR), and 1H and ^{13}C NMR techniques. The magnitude of the red shift of the C^2-H vibration mode of the imidazolium ring and the deshielding of the C^2-H hydrogen and carbon atoms, as a comparison with those of the other atoms of the ring or of the anion, indicated a strong interactions between the C^2-H hydrogen atom with the molecular liquids in the following order; DMSO \gg MeOH $>$ AN. This correlates with the order of the electron-donicties of these molecular liquids which allows us to suggest a hydrogen bonding character of these interactions. The behavior of S=O vibration of DMSO as a function of DMSO mole fraction x_{DMSO} also suggested that DMSO molecules are stoichiometrically hydrogen-bonded with the three hydrogen atoms, $C^{2,4,5}-H$ of the ring. In contrast, the hydrogen bonds between MeOH and the $C^{4,5}-H$ atoms are much weaker than those in DMSO. AN scarcely forms the hydrogen bonds with the $C^{4,5}-H$ atoms. Instead, AN molecules may interact with the imidazolium ring through the $\pi-\pi$ interaction. The interactions between the imidazolium ring and the molecular liquids lead to the loosening of TFSI anion from the cation; this correlates with both the blue-shift of the S=O stretching vibration of TFSI and the deshielding of the trifluoromethyl carbon atoms with increasing mole fraction of molecular liquid x_{ML} . The latter is weak in the MeOH solutions, and may be explained by the possible hydrogen bonding of the MeOH hydroxyl group as an electron-acceptor with TFSI anion. Furthermore, the organization of MeOH molecules around the ethyl and methyl groups of the cation is discussed in terms of the chemical shift of the hydrogen and carbon atoms within these groups as a function of x_{ML} .

1. Introduction

Ionic liquids are attractive as a novel reaction field because of their electroconductivity, negligible vapor pressure, and non-flammability. However, their high viscosity is the main disadvantage for their use in many applications. Mixing these ionic liquids with molecular solvents (protic and aprotic ones) is one of the ways to modulate the viscosity. Thus, the physicochemical properties of mixed solvents of imidazolium-based ionic liquid with various molecular liquids should be well understood to apply ionic liquid–molecular solvent mixture as a reaction medium (chemical synthesis, electrochemistry, and extraction). Particularly, it is interesting to analyze how the electrostatic interactions between cations and anions of the ionic liquids are affected by molecular liquid. Because the ring is positively charged, the hydrogen atoms of the imidazolium ring ($C^{2,4,5}\text{-H}$) may act as the hydrogen bond donors (the notation of all the atoms within the imidazolium ring is depicted in Fig. 1). In fact, the acidities of various imidazolium derivatives have been evaluated using probe molecules.^{1,2} In particular, the $C^2\text{-H}$ hydrogen atom has the highest acidity among the three hydrogen atoms.^{3,4}

The interactions between the $C^{2,4,5}\text{-H}$ hydrogen atoms of the imidazolium ring and molecular liquids have been already reported using IR spectroscopy. For 1-butyl-3-methylimidazolium tetrafluoroborate ($C_4\text{mimBF}_4$)–DMSO- d_6 solutions, two peaks at 3120 and 3160 cm^{-1} , which were assigned to the $C^2\text{-H}$ and $C^{4,5}\text{-H}$ stretching vibrations, respectively, gradually red-shift with increasing DMSO mole fraction.⁵ It has been concluded that the red-shift of the vibrations is attributed to the $C\text{-H}\cdots\text{O}$ hydrogen bonds between the imidazolium ring hydrogen and the DMSO oxygen atoms. The other IR investigation on the same system under GPa-pressures has also confirmed the hydrogen bonds between the imidazolium ring hydrogen atoms and the oxygen atom of DMSO.⁶ Recently, ATR-IR measurements have been made on $C_4\text{mimBF}_4$ –DMSO- d_6 solutions to derive the excess

spectra of the solutions. The hydrogen bonds between the imidazolium ring and DMSO were concluded from the red-shifts of the $C^{2,4,5}-H$ vibrations.⁷ In C_4mimBF_4 -MeOH- d_4 solutions, the C-H vibrations of the imidazolium ring red-shift as the MeOH concentration increases.⁸ The dissociation of C_4mim and BF_4 is facilitated on adding MeOH into the ionic liquid. In other words, MeOH molecules may interact with the imidazolium ring. The interactions between C_4mim and BF_4 are loosened by adding MeOH as a result of the preferential interaction between MeOH and the imidazolium ring. Ludwig and his coworkers have also investigated MeOH- d_4 solutions of 1-ethyl-3-methylimidazolium bis(trifluoromethanesulfonyl)imide ($C_2mimTFSI$) using ATR-IR spectroscopy.⁹ They have mainly discussed the formation of MeOH clusters in the solutions in terms of the O-H stretching vibrations of MeOH, but the details of the hydrogen bonds between the imidazolium ring and MeOH were not reported. In $C_2mimTFSI$ -AN- d_3 solutions, the C^2-H and $C^{4,5}-H$ vibrations of the imidazolium ring suggested that the inherent network structure of the ionic liquid is perturbed into ion pairs with the increase in both AN concentration and GPa-pressure.¹⁰ The other investigation on AN solutions of C_4mimBF_4 by ATR-IR and 1H NMR techniques showed that the hydrogen bond between the hydrogen atoms of the imidazolium ring and AN is strengthened with increasing AN concentration. Moreover, AN molecules may interact with the ring through the methyl group.¹¹ Molecular dynamics (MD) simulations have been performed on neat ionic liquids¹² of C_nmimPF_6 and $C_nmimTFSI$ with various alkyl chain lengths n and their mixtures with hexane, water, MeOH, and AN.^{13,14} In ionic liquids, microphase separation occurs, i.e., the imidazolium cations and anions form polar domains, while the alkyl chains self-aggregate and form nonpolar domains. In a mixture, water mainly exists in the polar domains, whereas hexane is preferentially localized in the nonpolar domains. MeOH and AN give the intermediate situation where they interact with

both polar and nonpolar domains. The MD simulations suggested that MeOH and AN interact with the imidazolium hydrogen atoms.

Despite the previous efforts, unknowns for the microscopic interactions of imidazolium-based ionic liquids with molecular liquids still remain. Particularly, the assignments of the C²-H and C^{4,5}-H vibrations modes of the imidazolium ring are still in controversy.^{15,16} In many investigations, the peaks at ~3120 and ~3160 cm⁻¹ were assigned to the C²-H and C^{4,5}-H stretching vibrations of the ring, respectively.¹⁷⁻¹⁹ However, according to the new assignments, the former arises from the Fermi resonance of the overtone associated with the in- and out-plane C-H bending vibrations of the ring, while the latter is attributed to the degenerated band of the C²-H and C^{4,5}-H vibrations.²⁰⁻²² Most of the investigations on imidazolium-based ionic liquid-molecular liquid solutions have been conducted using single technique, such as IR spectroscopy. The controversy on the assignment of C²-H and C^{4,5}-H vibrations modes of the imidazolium ring suggests that analyzing the hydrogen bonds between the imidazolium ring and molecular liquids using only the C-H stretching vibrations of the ring is not a straightforward task. Furthermore, the previous investigations have been individually made on one or two ionic liquid-molecular liquid systems, except for the MD simulations.^{13,14} Hence, the comparison between the effects of various molecular liquids on the C²-H and C^{4,5}-H vibrations modes of the imidazolium ring of the same IL have not yet been carried out.

Accordingly, in the present investigation, we use a multi-technical approach (Raman, IR and NMR) where each method opens a specific and complementary window on the interactions with the imidazolium-based ionic liquid of C₂mimTFSI (Fig. 1) and three molecular liquids including DMSO, MeOH, and AN. Indeed, ¹H and ¹³C NMR measurements were performed on the C₂mimTFSI-molecular liquid solutions, accompanied by Raman and ATR-IR spectroscopy particularly in the spectral region of the C-H vibration modes of the

imidazolium ring. Furthermore, the changes in the S=O vibrations of DMSO and TFSI anion in the solutions with increasing the mole fraction of DMSO x_{DMSO} were observed by means of ATR-IR to clarify the specific interaction of DMSO with the imidazolium ring and the loosening of TFSI from the cation. The behavior of the S=O vibration modes of DMSO and TFSI as a function of the concentration was used as an observable to clarify the interactions between the cation, the anion, and the molecular liquid.

The results suggest the correlation between the molecular liquids electron-donicity (Gutmann's donor numbers are 29.8, 19.0, and 14.1, for DMSO, MeOH and AN solvents, respectively²³) and their interactions with the imidazolium-based ionic liquid of C₂mimTFSI.

The paper is organized as follows: in the second section details are given on the experimental techniques used in this study. The third section constitutes the core of our paper where the behavior as a function of molecular liquid mole fraction x_{ML} of the stretching vibrations of the C–H of the cation, of the S=O of the anion and the solvent, the chemical shifts of the H and C atoms of the ring as well as those of the ethyl and methyl groups are presented and discussed and finally a conclusion is drawn to summarize our findings.

2. Experimental Section

2.1 Sample Solutions

C₂mimTFSI was synthesized with the conventional method previously reported.²⁴ Water content of C₂mimTFSI synthesized was determined to be less than 100 ppm by a Karl-Fisher titration. DMSO (Wako Pure Chemicals, grade for infinity pure) was dried on molecular sieves of 4 Å before use. MeOH (Wako Pure Chemicals, grade for HPLC) and AN (Wako Pure Chemicals, grade for HPLC) were used without further purification. All sample solutions were prepared by weighing C₂mimTFSI and the molecular liquid solvents at various x_{ML} in a nitrogen-filled glove box.

2. 2 Raman Spectroscopy

To observe the C–H stretching vibrations within the imidazolium ring in the C₂mimTFSI–DMSO solutions at a room temperature, Raman spectra were recorded using LabRam HR visible micro-Raman spectrometer (HORIBA Jobin Yvon), equipped with confocal microscope (50× magnifying objective was used), in back-scattering geometry in the spectral range 50–3500 cm⁻¹. Solid-state laser ($\lambda = 532$ nm) was used for excitation. Raman signal was collected with a CCD-detector (1024×256 pixels) placed after a diffraction grating (1800 grooves/mm) giving the final spectral resolution of about 0.3 cm⁻¹. The wavenumber scale was calibrated prior to every measurement series with a standard Si sample (520.7 cm⁻¹). Spectra were accumulated in a single scan with exposure time of 300 s per each orientation of the grating which assured sufficient use of sensitivity of the detector and reducing the background noise.

2. 3 ATR-IR Spectroscopy

ATR-IR experiments with a single reflectance were carried out on the C₂mimTFSI–DMSO, MeOH, and AN solutions over the entire x_{ML} range at a room temperature. An FT-IR spectrometer (JASCO, FT/IR-6100) equipped with ATR diamond prism (JASCO, PKS-D 470 with ATR PRO450-S) was utilized. The absorption spectra were accumulated with a wavenumber resolution of 4.0 cm⁻¹ for 32–512 times per sample depending on the concentrations of the target species. In the ATR-IR measurements on the S=O stretching vibrations of DMSO molecules, the wavelength dependence of the path length of irradiated light was corrected to determine the exact absorbance of the vibration bands. The absorption occurs in the evanescent wave penetrating into the sample, resulting in a decrease in the amplitude of irradiated light. The penetration depth d_p of the evanescent wave per reflection by a prism can be estimated through²⁵

$$d_p = \frac{\lambda}{2\pi} (n_1 \sqrt{\sin^2 \theta - n_2^2 / n_1^2})^{-1}. \quad (1)$$

Here, λ represents the wavelength of the light, θ is the incident angle (45°), n_1 and n_2 are the refractive indexes of diamond prism (2.42) and sample solution, respectively. In the present experiments, the refractive indexes of the sample solutions at 298 K were determined using a digital Abbe refractometer (ATAGO, DR-A1). Densities of the sample solutions were determined at 298.2 K with an electronic densimeter (Anton Paar GmbH, DSA5000) to estimate the molarities of C₂mimTFSI and DMSO for the sample solutions.

2. 4 NMR Spectroscopy

¹H and ¹³C NMR spectra of the C₂mimTFSI solutions with DMSO and AN at 298.2 K were recorded with varying x_{ML} on a 400 MHz FT-NMR spectrometer (Agilent Technologies, 400 MHz NMR system). ¹³C NMR spectra of the ionic liquid–MeOH solutions at 298.2 K were also measured at various mole fractions, whereas ¹H NMR data of them have already been reported in our previous investigation.²⁶ The digital resolutions of ¹H and ¹³C NMR measurements were 4.9×10^{-4} and 7.7×10^{-3} ppm, respectively. An external double reference tube (Shigemi), which has a capillary shape with a blown-up sphere at its base, was inserted into the sample tube (Shigemi, PS-001-7). Hexamethyldisiloxane (HMDS) (Wako Pure Chemicals, the first purity grade) was used as a reference substance for ¹H and ¹³C chemical shifts. The observed chemical shifts were corrected for the volume magnetic susceptibility of a sample solution using an external double reference method as described elsewhere.²⁷⁻³¹ During the NMR measurements, the sample temperature was controlled at 298.2 ± 0.1 K by a heater and a dry cold air from a sample cooler (FTS Systems, Air-Jet XR401, TC-84).

3. Results and Discussion

3. 1 The C–H stretching vibration modes of the imidazolium ring

Fig. 2 illustrates Raman spectra of the C₂mimTFSI–DMSO solutions at various x_{DMSO} . In the spectrum of C₂mimTFSI ($x_{\text{DMSO}} = 0$), a dominant peak appears at 3170 cm⁻¹, accompanied by several humps at the lower wavenumbers. The peak and the humps are assigned to the C²–H, C⁴–H and C⁵–H stretching vibration modes on the basis of the previous Raman investigations.^{22,32} However, the assignments of the modes are controversial as it will be shown below. The spectra of the solutions can be deconvoluted into four components using pseudo-Voigt functions as shown by the broken lines in Fig. 2. As observed in our Raman investigation on C₄mimPF₆– γ -butyrolactone solutions,³³ the two components at the lower wavenumbers often significantly red-shift as the concentration of molecular liquid increases rather than the other two components at the higher wavenumbers. In Fig. 3a and b, the wavenumbers of the components at 3121 and 3170 cm⁻¹ are plotted against the x_{DMSO} , respectively. The former more remarkably red-shifts with increasing DMSO concentration than the latter. The red-shifts of the C–H vibrations of the imidazolium ring with increasing x_{DMSO} show that the C–H bonds are weakened as the x_{DMSO} increases. Due to the strong electron-donicity of DMSO, the hydrogen-bond between the imidazolium ring hydrogen atoms and the oxygen atom of DMSO may be established.⁵⁻⁷ It is plausible that the most acidic C²–H atom^{3,4} is more strongly hydrogen-bonded with DMSO compared to the C⁴–H and C⁵–H atoms having lower acidity. Thus, the two components at the lower wavenumbers may be assigned to the C²–H stretching vibration, while the remaining two components at the high wavenumbers may arise from the C⁴–H and C⁵–H ones.

To more clearly elucidate the interactions between the imidazolium ring hydrogen atoms and the molecular liquids, ATR-IR experiments were conducted on the three systems as a function of x_{ML} . The spectra of the C–H stretching vibration modes within the imidazolium ring in mixtures with DMSO, MeOH, and AN are depicted in Fig. 4a, b, and c, respectively.

Two peaks appear at ~ 3125 and ~ 3157 cm^{-1} and are associated with $\text{C}_2\text{mimTFSI}$. These spectra were fitted using pseudo-Voigt functions to exactly determine the wavenumbers of the vibration modes. At the high x_{DMSO} , the C–H stretching vibrations of the DMSO methyl group contribute to the spectra in the low wavenumbers range and then there is no overlap between the spectral contributions of the ionic liquid and the DMSO solvent. At high x_{MeOH} , at the higher wavenumbers, the background rises due to the spectral contribution tail of the O–H stretching vibration of MeOH. The C–H vibration of the AN methyl group overlaps with that of the ionic liquid at around 3165 cm^{-1} . However, the relative intensity of this vibration mode is very small and was neglected in our study. As it was suggested in the previous investigations, the spectra for all the solutions below $x_{\text{ML}} = 0.9$ were deconvoluted by four spectral components.¹⁷⁻¹⁹

In Fig. 3c and d, the wavenumbers of the components at 3125 and 3157 cm^{-1} , associated with the C–H vibration modes of the ionic liquid, are plotted as a function of x_{ML} , respectively. Among the three molecular liquid solutions, the former significantly red-shifts with increasing x_{ML} in the DMSO solution. The latter also red-shifts with the increase in the x_{ML} however to a lesser extent. Based on the assignments of the components at 3125 and 3157 cm^{-1} to the $\text{C}^2\text{--H}$ and $\text{C}^{4,5}\text{--H}$ stretching vibrations of the ring, respectively,¹⁷⁻¹⁹ the red-shift of both peaks for the DMSO solutions suggests that DMSO molecules are hydrogen-bonded with the imidazolium ring hydrogen atoms. This interpretation is consistent with the red-shift of the $\text{C}^2\text{--H}$ and $\text{C}^{4,5}\text{--H}$ vibration modes observed by Raman spectroscopy. The hydrogen bond of DMSO with the $\text{C}^2\text{--H}$ atom is stronger compared to those with the $\text{C}^4\text{--H}$ and $\text{C}^5\text{--H}$ atoms due to the high acidity, as described above. Based on the new assignments,²⁰⁻²² the 3157 cm^{-1} component arises from all the degenerated C–H vibration modes and the red-shift of the component at 3157 cm^{-1} then implies that DMSO establishes hydrogen bond with all the hydrogen atoms of the imidazolium ring. On the contrary, the

component at 3125 cm^{-1} is attributed to the Fermi resonance of the overtone for the in- and out-plane C–H bending vibrations of the imidazolium ring. In Fig. 4d, the spectra associated with the in- and out-plane C–H bending band at around 1574 cm^{-1} for the DMSO solutions is depicted as a function of x_{DMSO} . A hump also appears at $\sim 1600\text{ cm}^{-1}$. The intensity of this peak with the hump decreases with increasing x_{ML} . However, the peak and the hump hardly shift with the increase in the x_{ML} , although the peak at 3125 cm^{-1} assigned to the Fermi resonance markedly shifts toward the lower wavenumber with increasing x_{ML} (Fig. 4a). Thus, we believe that the component at 3125 cm^{-1} includes the information on the hydrogen bond of the ring hydrogen atoms with DMSO. Fig. 3c and d show that the component at 3125 cm^{-1} for the MeOH solutions slightly red-shifts with the increase in the x_{ML} , whereas the component at 3157 cm^{-1} scarcely shifts against the x_{ML} . Both components for the AN solutions hardly change with increasing x_{ML} . As shown in Fig. 4e and f, the in- and out-plane C–H bending band at 1574 cm^{-1} for both MeOH and AN solutions does not shift with increasing x_{ML} , as well as that for the DMSO solutions. These results indicate that the in- and out-plane C–H bending vibrations are not sensitive to the hydrogen bonding of the imidazolium ring hydrogen atoms.

If the components at 3125 and 3157 cm^{-1} are ascribed to the $\text{C}^2\text{-H}$ and $\text{C}^{4,5}\text{-H}$ stretching vibrations, respectively,¹⁷⁻¹⁹ the present results show that the $\text{C}^2\text{-H}$ atom with the higher acidity is very weakly hydrogen-bonded with MeOH, while the $\text{C}^{4,5}\text{-H}$ atoms with the lower acidity are not significantly bound to MeOH. In contrast, the ring hydrogen atoms scarcely form the hydrogen bonds with AN. Even if the new assignments are adopted, we can conclude from the red-shift of the component at 3157 cm^{-1} that the imidazolium ring hydrogen atoms are strongly hydrogen-bonded with DMSO, which is consistent with the high electron-donicity of DMSO.

3. 2 ^1H and ^{13}C NMR chemical shifts of C_2mim cation

Fig. 5a and b show the representative ^1H and ^{13}C NMR spectra of the $\text{C}_2\text{mimTFSI-DMSO}$ solutions as a function of the DMSO mole fraction, respectively, as well as the assignments of the observed peaks.³⁴ Most of the peaks of C_2mim cation shift toward the low magnetic field with increasing DMSO concentration. The ^1H and ^{13}C NMR peaks for the MeOH and AN solutions also shift to the low field as the x_{ML} increases, except for a few peaks (see discussion later).

In Fig. 6, the corrected NMR chemical shifts of the hydrogen and carbon atoms within the imidazolium ring in the three $\text{C}_2\text{mimTFSI-molecular liquid}$ systems are plotted against the x_{ML} . The ^1H NMR data for the MeOH solutions in the figure have already been reported in our previous investigation.²⁶ The $\text{C}^2\text{-H}$ atoms of the imidazolium ring in the DMSO solutions are significantly deshielded with increasing x_{ML} . In addition, the $\text{C}^{4,5}\text{-H}$ atoms are also deshielded as the x_{ML} increases. The magnitudes of the deshielding for the atoms at the positions 4 and 5 are comparable with each other, but weaker than that of the $\text{C}^2\text{-H}$ atoms. In the MeOH solutions, the deshielding of the $\text{C}^2\text{-H}$ atoms is much weaker compared to that of the DMSO solutions. The $\text{C}^{4,5}\text{-H}$ atoms in the MeOH solutions are more weakly deshielded as the x_{ML} increases compared to the $\text{C}^2\text{-H}$ atoms. These NMR features for the DMSO and MeOH solutions thoroughly agree with the red-shifts of the Raman and IR components at the higher and lower wavenumbers against the increase in the x_{ML} (Fig. 3). The NMR results, together with the C-H stretching vibrations, confirm the occurrence of the hydrogen bonds of the imidazolium ring hydrogen atoms with DMSO and MeOH. These results also prove that DMSO molecules are more strongly hydrogen-bonded with the $\text{C}^2\text{-H}$ than with the $\text{C}^{4,5}\text{-H}$ atoms. The hydrogen bond between MeOH molecule and the $\text{C}^2\text{-H}$ atom is weaker compared to that with DMSO. The $\text{C}^{4,5}\text{-H}$ atoms are less significantly bound to MeOH. For the AN

solutions, the deshielding of the C²-H atoms against the increase in the x_{ML} is the weakest among the three systems. This is also comparable with the magnitude of the red-shift for the IR component at $\sim 3125\text{ cm}^{-1}$. Thus, the hydrogen bond between the C²-H atom of the imidazolium ring and the molecular liquids is stronger in the order of DMSO \gg MeOH $>$ AN. This correlates with the order of the electron-donicities of the three molecular liquids.²³ The chemical shifts of the C^{4,5}-H hydrogen atoms in the MeOH and AN solutions almost overlap with each other. This is consistent with the behavior of the IR component at $\sim 3157\text{ cm}^{-1}$. AN and MeOH molecules do not significantly interact with the C^{4,5}-H hydrogen atoms. However, the deshielding of the C⁴ and C⁵ carbon atoms in the AN solutions with the increase in the x_{ML} is slightly higher compared to that in the MeOH solutions. Probably, the deshielding field along the C \equiv N bond of AN molecule influences the carbon atoms at the positions 4 and 5. Thus, the π - π interaction may act between the imidazolium ring and AN molecule.

Fig. 7 illustrates the behavior of the chemical shifts of the hydrogen and carbon atoms within the ethyl and methyl groups of C₂mim in the three systems as a function of x_{ML} . The ethyl and methyl hydrogen atoms in all of the systems are deshielded with the increase in the molecular liquid concentration. The deshielding of the alkyl hydrogen atoms is much weaker compared to the imidazolium ring hydrogen atoms even for the DMSO solutions. A similar weak deshielding of the alkyl hydrogen atoms with increasing MeOH mole fraction were also observed for C₄mimBF₄-MeOH solutions.³⁵ On the other hand, the changes in the chemical shifts of the ethyl and methyl carbon atoms in the three systems with increasing x_{ML} have a particular behavior. The ¹³C NMR chemical shifts are more sensitive to the type of the molecular liquids compared to the ¹H NMR data. This may arise from the redistribution of electron density within the skeletal carbon atoms of the imidazolium cation. The methylene carbon C⁶ atom of the ethyl group is slightly deshielded in the DMSO solutions with

increasing x_{ML} . The deshielding of the C^6 atom in the AN solutions with the increase in the x_{ML} is higher compared to that in the DMSO solutions despite the stronger hydrogen bonds of the ring hydrogen atoms with DMSO. In contrast, the C^6 atom in the MeOH solutions is slightly shielded above $x_{ML} \approx 0.8$. Interestingly, the terminal methyl carbon C^7 atom of the ethyl group in the DMSO solutions is strongly deshielded with increasing x_{ML} compared to that in the AN solutions, although the deshielding of the C^6 atom in the former is weaker than that in the latter. The chemical shift of the C^7 atom in the MeOH solutions scarcely changes as the mole fraction of the molecular liquid increases. The C^8 atom of the methyl group bound to the nitrogen N^3 atom is deshielded in the DMSO and AN solutions against the increase in the x_{ML} , as well as the C^7 atom. However, the C^8 atom in the MeOH solutions is shielded with increasing x_{ML} .

The deshielding of the C^6 , C^7 , and C^8 atoms in the DMSO and AN solutions may be related to the magnitude of the interactions between the imidazolium ring and DMSO or AN. As discussed above, DMSO molecules are strongly hydrogen-bonded with the ring hydrogen atoms. This leads to the redistribution of electron density of the ethyl and methyl carbon atoms, i.e. the electron densities of the C^7 and C^8 atoms significantly decrease in the DMSO solutions with increasing x_{ML} . In the AN solutions, the redistribution of electron densities of both C^7 and C^8 atoms is less significant than that in the DMSO solutions because of the weaker interaction between the imidazolium ring and AN. The other plausible reason for the deshielding of the alkyl carbon atoms of C_2mim is the interactions between the alkyl groups and the DMSO $S=O$ and AN $C\equiv N$ groups. Both $S=O$ and $C\equiv N$ groups might induce the deshielding of the alkyl carbon atoms due to their deshielding field along the bond axis.

The changes in the chemical shifts of the C^6 , C^7 , and C^8 atoms in the MeOH solutions with increasing x_{ML} are obviously different from those in the DMSO and AN solutions. The chemical shift of the C^7 atom is almost constant against the increase in the x_{ML} . The C^8 atom

is shielded with increasing x_{ML} . In addition, the C⁶ atom is slightly shielded above $x_{ML} \approx 0.8$. These features may be ascribed to the self-aggregation of MeOH molecules through hydrogen bonding as reported in our previous investigations using a small-angle neutron scattering (SANS) technique.^{26,36} The SANS spectra of C_nmimTFSI–MeOH-*d*₄ solutions with the alkyl chain length of $n = 2–12$ showed the heterogeneous mixing of both liquids above $x_{MeOH} \approx 0.8$ because MeOH molecules self-aggregate by hydrogen bonding in C_nmimTFSI. Indeed, the IR investigation by Ludwig et al.⁹ indicated that MeOH molecules are hydrogen-bonded with themselves to form aggregates in C₂mimTFSI. When MeOH molecules aggregate through the hydrogen bonds involving the hydroxyl groups, the methyl groups are oriented toward the outside of the aggregate. Hence, the methyl groups of the MeOH clusters around the imidazolium may interact with the ethyl and methyl groups of the imidazolium through the dispersion force. The same shielding of the imidazolium methyl group was observed in the previous investigation on MeOH solutions of C_nmimTFSI with $n = 4–12$.³⁶ In fact, the previous IR investigation on C₄mimBF₄–MeOH-*d*₄ solutions showed that the alkyl C–H stretching vibration of C₄mim cation blue-shifts with increasing MeOH concentration above $x_{MeOH} \approx 0.9$.⁸ The shortening of the C–H bonds leads to the increase in the electron density of the alkyl carbon atoms of the imidazolium.

3. 3 The S=O stretching vibration modes of DMSO

The ATR-IR spectra of the S=O stretching vibration modes of DMSO molecule in the C₂mimTFSI–DMSO solutions as a function of x_{DMSO} are shown in Fig. 8a. The spectra were corrected for the penetration depth of the irradiation light into the solutions on the diamond prism to determine the exact absorbance of the vibration as described in the experimental section. An isosbestic point is found at 1045 cm⁻¹, suggesting that two species mainly coexist in the solutions. A peak centered at 1051 cm⁻¹ arises from C₂mimTFSI. Indeed, this peak most strongly appears at $x_{DMSO} = 0$ and gradually weakens as the x_{DMSO} increases. A peak at

1042 cm^{-1} and a shoulder at $\sim 1020 \text{ cm}^{-1}$ arise from the S=O vibrations of DMSO.³⁷ The intensities of these two peaks increase with increasing x_{DMSO} . To extract the S=O vibrations of DMSO alone, the spectrum of C₂mimTFSI was subtracted from the original spectra of the DMSO solutions with taking into account of the molarity of the ionic liquid. The difference spectra of the solutions, where the S=O vibrations of DMSO contribute, are indicated in Fig. 8b. Several peaks appear in the difference spectrum of DMSO. Based on the previous report,³⁷ the shoulder at 1055 cm^{-1} is assigned to the S=O vibration of DMSO monomer, while the peak at 1042 cm^{-1} and the shoulder at $\sim 1020 \text{ cm}^{-1}$ are attributed to the asymmetric and symmetric vibrations of DMSO dimer, respectively, where DMSO molecules may interact with each other by the dipole–dipole interactions between the S=O moieties.

Although the difference spectra show the mole fraction dependence of the S=O vibrations of DMSO, the state of DMSO molecules in the solutions cannot be easily explained on the basis of the change in the difference spectra with the increase in the DMSO concentration. Therefore, the spectrum of DMSO weighed by the corresponding concentration was further subtracted from the difference spectra of the solutions. In Fig. 8c, the double difference spectra of the DMSO solutions are shown with varying x_{DMSO} . The negative peak at $\sim 1051 \text{ cm}^{-1}$ indicates the decrease in the concentration of DMSO monomers in the solutions from that in pure DMSO. In contrast, two peaks at ~ 1042 and $\sim 1018 \text{ cm}^{-1}$ reveal the increase in the concentration of DMSO dimers with respect to that in pure DMSO. A peak at $\sim 1028 \text{ cm}^{-1}$ can be attributed to the S=O vibration of DMSO hydrogen-bonded with the imidazolium ring in the solutions.

In Fig. 9, the negative and positive values of absorbance at ~ 1051 and $\sim 1028 \text{ cm}^{-1}$, respectively, are plotted against x_{DMSO} . The negative absorbance for DMSO monomer gradually decreases with increasing x_{DMSO} to 0.7 and then increases with the further increase in the DMSO concentration. This finding suggests that there are less DMSO monomers in the

solutions below $x_{\text{DMSO}} = 0.7$ compared to that in pure DMSO, but the concentration of DMSO monomer gradually recovers in the solutions with increasing x_{DMSO} from 0.7 to 0.99. On the contrary, the positive absorbance for the hydrogen-bonded DMSO increases as the x_{DMSO} increases up to 0.7 and then decreases with further increasing x_{DMSO} below 0.99. The mole fraction of $x_{\text{DMSO}} = 0.7$ for the inflection points is close to the ratio 1:3 of one imidazolium ring with the three hydrogen bonding sites to three DMSO molecules, which corresponds to $x_{\text{DMSO}} = 0.75$. Thus, DMSO molecules added to the ionic liquid are stoichiometrically hydrogen-bonded with the three hydrogen atoms of the ring. In the solutions, the concentration of DMSO monomers increases with increasing x_{DMSO} from ~ 0.7 due to the saturation of the hydrogen bonding sites of the imidazolium ring. These results on the hydrogen bond acceptor of the DMSO S=O group are consistent with those on the hydrogen bond donors of the imidazolium ring C–H groups as discussed above.

3.4 The S=O stretching vibration modes and the ^{13}C NMR chemical shift of TFSI anion

The previous investigation on $\text{C}_2\text{mimTFSI}$ by X-ray diffraction with a help of MD simulations showed that TFSI anions interact with the imidazolium ring at the positions 2, 4, and 5.³⁸ Particularly, TFSI distributes around the position 2 with the highest probability among the three sites of the ring. The far-infrared spectroscopic measurements on $\text{C}_2\text{mimTFSI}$ also suggested that the interaction between TFSI and the ring at the position 2 is stronger compared to that at the positions 4 and 5.³⁹ Therefore, as the molecular liquids interact with the imidazolium ring, the interaction between TFSI and the ring should be weakened, particularly at the position 2. Fig. 10 indicates the ATR-IR spectra for the in- and out-phase asymmetric S=O stretching vibrations of TFSI at 1350 and 1330 cm^{-1} , respectively,⁴⁰ in the $\text{C}_2\text{mimTFSI}$ –molecular liquid solutions with varying x_{ML} . The S=O vibrations of TFSI for all of the solutions gradually blue-shift with increasing x_{ML} . This suggests that the S=O bond becomes stronger as the x_{ML} increases. In other words, TFSI

anions are loosened from the imidazolium ring as a result of the interactions between the imidazolium ring and molecular liquids. The S=O vibration band of TFSI was fitted using pseudo-Voigt functions to determine the wavenumber of the vibration.

In Fig. 11, the wavenumbers of the in-phase asymmetric S=O vibration of TFSI in the three systems are plotted against x_{ML} . The S=O vibration of TFSI in the DMSO solutions most significantly blue-shifts with increasing x_{ML} among the three systems. This is reasonable with the strongest hydrogen bonds of the imidazolium ring hydrogen atoms with DMSO. However, the blue-shift of the S=O vibration is not large even in the DMSO solutions. The effect of DMSO on the asymmetric S=O vibration modes of TFSI as well as on the chemical shift of the C^{2,4,5}-H of the imidazolium ring suggests the physical picture that in neat ionic liquids, the TFSI is widely distributed around the positions 2, 4, and 5 of the imidazolium ring and although the interaction between the S=O of TFSI and the hydrogen atoms of the imidazolium ring may be considered as electrostatic, it did not have a preferential direction such as in the case of a linear strong hydrogen bond configuration Y...H-X.^{38,41,42} Thus, the S=O bonds of TFSI are not strongly affected by the imidazolium ring even in the neat ionic liquid. It results in the small blue-shift of the S=O vibration as the interaction between the ring and TFSI anions is loosened with increasing x_{ML} .

The blue-shifts of the S=O vibration of TFSI in the MeOH and AN solutions with increasing x_{ML} are comparable with each other, although the interaction of the position 2 of the imidazolium ring with MeOH is stronger than that with AN, as shown in Figs. 3 and 6. This is because MeOH molecules may be hydrogen-bonded with TFSI anions that are loosened from the imidazolium ring. The hydroxyl hydrogen moiety of MeOH acts as a hydrogen bond donor to the TFSI oxygen atoms with the $D_N = 7$.^{43,44} Actually, the electron-acceptability of MeOH is much higher than DMSO and AN, as seen by the Mayer-Gutmann's acceptor numbers of $A_N = 41.3, 19.3, \text{ and } 19.3$, respectively.²³

The blue-shift of the TFSI S=O vibration in the MeOH solutions above $x_{ML} \approx 0.8$ may be related to the aggregation of MeOH molecules in the solutions. As described above, MeOH molecules self-aggregate in $C_n\text{mimTFSI}$ with $n = 2-12$,^{9,26,36} i.e., the ionic liquids and MeOH are heterogeneously mixed each other. The heterogeneity of the MeOH solutions is enhanced above $x_{\text{MeOH}} \approx 0.8$. This agrees with the mole fraction where the blue-shift of the S=O vibration of TFSI becomes significant for the MeOH solutions with increasing x_{ML} . The hydrogen bond between TFSI and MeOH may be weakened because of the self-aggregation of MeOH molecules.

Fig. 12 shows the chemical shifts of the trifluoromethyl carbon atoms within TFSI in the three systems as a function of x_{ML} . The carbon atoms of TFSI are gradually deshielded in the DMSO and AN solutions against the increase in the x_{ML} . The deshielding of the carbon atoms in the DMSO and AN systems is ascribed to the weakening of the interaction between TFSI and the imidazolium ring. The previous investigation revealed that the TFSI carbon and fluorine atoms in $C_2\text{mimTFSI}$ are deshielded with temperature to 313 K due to the loosening of the inherent structure of $C_2\text{mimTFSI}$.³⁸ The long-range ordering are observed even in the neat ionic liquid. Hence, TFSI is close to the nearest neighbor TFSI which is ~ 9 Å apart.³⁸ Probably, the trifluoromethyl groups of two TFSI anions interact with each other because the negatively charged $\text{N}(\text{SO}_2)_2^-$ moiety of TFSI may mainly orient to the imidazolium ring. The dispersion force may act between the trifluoromethyl groups. This leads to the high electron density of the trifluoromethyl carbon atoms in the neat ionic liquid, as shown in the interactions of the alkyl groups of organic solutes with fluorinated alcohols.⁴⁵⁻⁴⁸ However, the interactions between the trifluoromethyl groups of TFSI anions are weakened as a result of the strengthening the interaction between the imidazolium ring and the molecular liquids with increasing x_{ML} . Thus, the electron density of the trifluoromethyl carbon atoms gradually decreases as the x_{ML} increases. The more significant deshielding of the TFSI carbon atoms for

the DMSO system than the AN one is related to the stronger interaction of the imidazolium ring with DMSO. On the contrary, the deshielding of the TFSI carbon atoms in the MeOH solutions with increasing x_{ML} is very weak, although the interaction between TFSI and the imidazolium ring should loosen as a result of the hydrogen bonds of the ring with MeOH molecules. The very weak deshielding of the trifluoromethyl carbon atoms of TFSI in the MeOH solutions is consistent with the results on the TFSI S=O vibration (Fig. 11). As discussed above, the weak deshielding of the trifluoromethyl carbon atoms may be caused by the hydrogen bonds between TFSI and MeOH molecules. The hydrogen bonds between TFSI and MeOH may cancel out the electron density redistribution of the trifluoromethyl carbon atoms of TFSI by loosening the interactions between TFSI and the imidazolium ring in the solutions with increasing x_{ML} . Thus, the chemical shift of the TFSI carbon atoms almost remains unchanged against the increase in the x_{ML} . TFSI anions loosened from the ring may interact with DMSO and AN molecules through the dipole-dipole interaction between them due to the large dipole moments of TFSI in the cis form,⁴⁹ DMSO, and AN (14.69×10^{-30} , 13.00×10^{-30} , and 13.06×10^{-30} Cm, respectively). In comparison, the dipole moment of MeOH (5.63×10^{-30} Cm) is the smallest.

3. 5 Discussion of the Interactions between C₂mim, TFSI, and molecular liquids

The assignments of the Raman and IR peaks at the lower and higher wavenumbers for the C–H stretching vibrations within the imidazolium ring are still controversial.^{15,16} Nevertheless, the present results suggest that both peaks may give us the information on the interaction between the ring hydrogen atom and the molecular liquids. In particular, the remarkable red-shift of the component at the lower wavenumber with increasing x_{ML} is observed for the DMSO solutions, although the component might be assigned to the Fermi resonance of the overtone for the C–H bending vibrations that hardly shift against the increase in the x_{ML} and are then not sensitive to the hydrogen bond interactions²⁰⁻²² The

hydrogen bonding of the imidazolium C²-H hydrogen atom with DMSO is strongly possible because of the high acidity of the C²-H atom and the high electron-donicity of DMSO. Actually, the dissociation constants of the C²-H atom within the various imidazolium derivatives have been evaluated in DMSO.³ Moreover, the changes in the Raman and IR components at the lower and higher wavenumbers against the x_{ML} are consistent with those in the ¹H and ¹³C NMR chemical shifts of the positions 2, 4, and 5 of the imidazolium ring.

Thus, according to the Raman, ATR-IR and NMR results, we conclude that the molecular liquids examined are more strongly hydrogen-bonded with the highly acidic C²-H atom of the imidazolium ring in the order of DMSO >> MeOH > AN. This correlates with the electron-donicities of the molecular liquids. DMSO with the highest electron-donicity among the molecular liquids also acts to the C⁴-H and C⁵-H hydrogen atoms of the imidazolium ring as a hydrogen bond acceptor. The hydrogen bonds of DMSO with the three hydrogen atoms of the imidazolium ring are reflected to the S=O stretching vibrations of DMSO. The S=O stretching vibrations show that the hydrogen-bonded DMSO molecules are gradually accumulated in the solutions with increasing x_{DMSO} to 0.7. On the contrary, the spectral contribution of the isolated DMSO monomers decrease until $x_{DMSO} = 0.7$, and then increase for the subsequent mole fractions. This behavior at $x_{DMSO} = 0.7$ suggests that DMSO molecules added into the ionic liquid are stoichiometrically hydrogen-bonded with the three hydrogen atoms of the imidazolium ring because the ratio of one imidazolium ring to three DMSO molecules corresponds to $x_{DMSO} = 0.75$.

In contrast to DMSO, the hydrogen bonds of MeOH molecules with the C^{4,5}-H hydrogen atom of the imidazolium ring are much weaker. Acetonitrile molecules are scarcely hydrogen-bonded with the C^{4,5}-H hydrogen atoms. This is because both the electron-donicities of the two molecular liquids are not as strong as that of DMSO and the acidity of the imidazolium C^{4,5}-H atoms is low. However, the ¹³C NMR data of the C⁴ and C⁵ atoms

suggest that AN molecule may interact with the imidazolium ring at the positions 4 and 5 through the π - π interaction between them.

The interaction between the imidazolium ring and the molecular liquids leads to the loosening of TFSI from the ring because TFSI anions weakly interact with the ring in $C_2mimTFSI$.^{38,41,42} The asymmetric S=O vibration of TFSI and the ^{13}C NMR chemical shifts clearly show the loosening of the interaction between TFSI and the imidazolium ring. The S=O bonds of TFSI are strengthened with increasing x_{ML} . Simultaneously, the trifluoromethyl carbon atoms of TFSI are gradually deshielded as the x_{ML} increases. This may be because the strengthening of the interaction between the imidazolium ring and the molecular liquids with increasing x_{ML} wedges the inherent interaction of TFSI with the nearest neighbor of TFSI in the ionic liquid. This leads to the decrease in the electron density of the trifluoromethyl carbon atoms. Both blue-shift and deshielding of TFSI in the DMSO solutions are the most significant among the molecular liquid solutions examined. This also suggests the strong hydrogen bonds between the imidazolium ring and DMSO.

TFSI loosened from the imidazolium ring as a result of the interaction between the imidazolium ring and the molecular liquids should also interact with the molecular liquids. DMSO and AN have the large dipole moment as well as TFSI in the cis form.⁴⁹ Thus, TFSI may be solvated by DMSO and AN molecules through the dipole-dipole interaction between them. In contrast, MeOH does not have the large dipole moment, but involves the high electron-acceptability of the hydroxyl hydrogen atom. The oxygen atoms of the TFSI S=O groups may be hydrogen-bonded with MeOH.⁴³ The hydrogen bonds between TFSI and MeOH are reflected in the weak blue-shift of the TFSI S=O vibration despite the weakening of the interaction between TFSI and the ring with increasing x_{ML} . The two factors can be considered as the reasons why the molecular liquids, particularly, DMSO molecules can be hydrogen-bonded with the imidazolium ring hydrogen atoms against the stronger electrostatic

force between the cation and the anion. The factor on the macroscopic scale is the reduction of the electrostatic force between both ions on adding the molecular liquids studied due to their high dielectric constant ($\epsilon_r = 46.6, 32.6, \text{ and } 35.95$ at 298 K for DMSO, MeOH, and AN, respectively). As a result, the interaction energies cation–anion and cation–solvent become comparable which allows effective competition between the two. The other factor on the microscopic scale is that the molecular liquids can interact with not only the cation but also the anion as described above. The two factors are the same in the dissolution of conventional salts like sodium chloride in polar molecular liquids.

In the neat ionic liquid, the imidazolium rings and TFSI may form the polar domains as shown in the previous MD investigation.¹² Thus, when the molecular liquids are added into the ionic liquid, all of the molecular liquids enter into the polar domain consisting of the imidazolium ring and TFSI through the hydrogen bond, the π – π interaction, and the dipole–dipole interaction. In the mixing between C₂mimTFSI and the molecular liquids, only MeOH molecule can be hydrogen-bonded with themselves due to both hydroxyl hydrogen and oxygen atoms. Thus, MeOH molecules easily self-aggregate by the hydrogen bonds to form MeOH clusters in the solutions above $x_{\text{MeOH}} \approx 0.8$.^{9,26,36} This is because the hydroxyl hydrogen atom of MeOH prefers the hydroxyl oxygen atom of them rather than TFSI due to the higher electron-donicity of MeOH. In fact, the previous SANS investigations²⁶ showed that C₂mimTFSI–MeOH solutions are heterogeneous on the mesoscopic scale due to hydrogen-bonded MeOH clusters, while AN molecules that weakly interact with themselves through the dipole–dipole interaction⁵⁰ are homogeneously mixed with C₂mimTFSI. Consequently, the mixing state of ionic liquid and molecular liquid is affected by not only the interactions of molecular liquid with the imidazolium ring and anion, but also the interactions among molecular liquids.

4. Conclusion

The C–H stretching vibrations and ^1H and ^{13}C NMR chemical shifts of the imidazolium ring of $\text{C}_2\text{mimTFSI}$ in mixtures with various molecular liquids show that the highly acidic $\text{C}^2\text{--H}$ atom of the imidazolium ring is more strongly hydrogen-bonded with the molecular liquids in the order of $\text{DMSO} \gg \text{MeOH} > \text{AN}$. Thus, the hydrogen bond depends on the electron-donicity of the molecular liquids. DMSO molecule with the high electron-donicity also forms the hydrogen bonds with the $\text{C}^{4,5}\text{--H}$ atoms of the imidazolium ring. The three hydrogen atoms of the imidazolium ring are stoichiometrically hydrogen-bonded with DMSO molecules. However, the hydrogen bonds of the $\text{C}^{4,5}\text{--H}$ atoms with MeOH are much weaker compared to DMSO. Acetonitrile molecules are scarcely hydrogen-bonded with the $\text{C}^{4,5}\text{--H}$ hydrogen atoms, but may interact with the positions 4 and 5 of the ring through the $\pi\text{--}\pi$ interaction. The inherent interaction between TFSI anions and the imidazolium ring in the ionic liquid is most remarkably loosened in the DMSO solutions among the three systems. This results from the stronger interaction between the ring and the molecular liquids in the above order. In the DMSO and AN solutions, TFSI anions loosened from the imidazolium ring may be solvated by the molecular liquids through the dipole–dipole interaction between them. On the contrary, TFSI anion can be hydrogen-bonded with MeOH molecules.

Acknowledgement

This work was supported partly by Grants-in-Aid for Scientific Research (C) (No. 22550018 and 26410018) from the Japan Society for the Promotion of Science and Dean's Grant for Progressive Research Projects from Saga University. T. T. conducted partly this work as an invited professor of the University of Lille 1, France. The NMR and density measurements for the sample solutions were made at the Analytical Research Center for Experimental Sciences of Saga University.

References

- 1 Y. Chu, H. Deng and J.-P. Cheng, *J. Org. Chem.*, 2007, **72**, 7790–7793.
- 2 S. Spange, R. Lungwitz and A. Schade, *J. Mol. Liquids*, 2014, **192**, 137–143.
- 3 A. Elaiwi, P. B. Hitchcock, K. R. Seddon, N. Srinivasan, Y.-M. Tan, T. Welton and J. A. Zora, *J. Chem. Soc., Dalton Trans.*, 1995, 3467–3472.
- 4 C. Hardacre, J. D. Holbrey, S. E. J. McMath, D. T. Bowron and A. K. Soper, *J. Chem. Phys.*, 2003, **118**, 273–278.
- 5 L. Zhang, Y. Wang, Z. Xu and H. Li *J. Phys. Chem., B*, 2009, **113**, 5978–5984.
- 6 J.-C. Jiang, K.-H. Lin, S.-C. Li, P.-M. Shih, K.-C. Hung, S. H. Lin and H.-C. Chang, *J. Chem. Phys.*, 2011, **134**, 044506-1–8.
- 7 Y.-Z. Zheng, H.-Y. He, Y. Zhou and Z.-W. Yu, *J. Mol. Structure* 2014, **1069**, 140–146.
- 8 H.-C. Chang, J.-C. Jiang, Y.-C. Liou, C.-H. Hung, T.-Y. Lai and S. H. Lin, *J. Chem. Phys.*, 2008, **129**, 044506-1–6.
- 9 C. Roth, A. Appelhagen, N. Jobst and R. Ludwig, *ChemPhysChem*, 2012, **13**, 1708–1717.
- 10 Y. Umebayashi, J.-C. Jiang, K.-H. Lin, Y.-L. Shan, K. Fujii, S. Seki, S. Ishiguro, S. H. Lin and H.-C. Chang, *J. Chem. Phys.*, 2009, **131**, 234502-1–7.
- 11 Y.-Z. Zheng, N.-N. Wang, J.-J. Luo, Y. Zhou and Z.-W. Yu *Phys. Chem. Chem. Phys.*, 2013, **15**, 18055–18064.
- 12 J. N. A. C. Lopes and A. A. H. Pádua, *J. Phys. Chem. B*, 2006, **110**, 3330–3335.
- 13 J. N. C. Lopes, M. F. C. Gomes and A. A. H. Pádua, *J. Phys. Chem. B (Letter)*, 2006, **110**, 16816–16818.
- 14 A. A. H. Pádua, M. F. C. Gomes and J. N. C. Lopes, *Acc. Chem. Res.*, 2007, **40**, 1087–1096.

- 15 A. Wulf, K. Fumino and R. Ludwig, *J. Phys. Chem. A*, 2010, **114**, 685–686.
- 16 J.-C. Lassègues, J. Grondin, D. Cavagnat and P. Johansson, *J. Phys. Chem. A*, 2010, **114**, 687–688.
- 17 T. Köddermann, C. Wertz, A. Heintz and R. Ludwig, *ChemPhysChem*, 2006, **7**, 1944–1949.
- 18 A. Wulf, K. Fumino, D. Michalik and R. Ludwig, *ChemPhysChem*, 2007, **8**, 2265–2269
- 19 A. Yokozeki, D. J. Kasprzak and M. B. Shiflett, *Phys. Chem. Chem. Phys.*, 2007, **9**, 5018–5026
- 20 J.-C. Lassègues, J. Grondin, D. Cavagnat and P. Johansson, *J. Phys. Chem. A* (Letter), 2009, **113**, 6419–6421.
- 21 T. Buffeteau, J. Grondin, Y. Danten and J.-C. Lassègues, *J. Phys. Chem. B*, 2010, **114**, 7587–7592.
- 22 J. Grondin, J.-C. Lassègues, D. Cavagnat, T. Buffeteau, P. Johansson and R. Holomb, *J. Raman Spectrosc.*, 2011, **42**, 733–743.
- 23 V. Gutmann, *The Donor–Acceptor Approach to Molecular Interactions*, Plenum Press, New York, 1978.
- 24 P. Nockemann, K. Binnemans and K. Driesen, *Chem. Phys. Lett.*, 2005, **415**, 131–136.
- 25 J. E. Bertie and H. H. Eysel, *Appl. Spectrosc.*, 1985, **39**, 392–401.
- 26 T. Takamuku, Y. Honda, K. Fujii and S. Kittaka, *Anal. Sci.*, 2008, **24**, 1285–1290.
- 27 T. Shimomura, T. Takamuku and T. Yamaguchi, *J. Phys. Chem. B*, 2011, **115**, 8518–8527.
- 28 K. Mizuno, Y. Tamiya and M. Mekata, *Pure Appl. Chem.*, 2004, **76**, 105–114.
- 29 K. Mizuno, S. Imafuji, T. Ochi, T. Ohta and S. Maeda, *J. Phys. Chem. B*, 2000, **104**, 11001–11005.
- 30 K. Momoki and Y. Fukazawa, *Anal. Chem.*, 1990, **62**, 1665–1671.

- 31 K. Momoki and Y. Fukazawa, *Anal. Sci.*, 1994, **10**, 53–58.
- 32 J. Kiefer, J. Fries and A. Leipertz, *Appl. Spectrosc.*, 2007, **61**, 1306–1311.
- 33 B. A. Marekha, M. Moreau, V. A. Koverga, M. Kiselev, T. Takamuku, O. N. Kalugin and A. Idrissi, *J. Raman Spectrosc.* submitted.
- 34 B.-M. Su and Z. C. Zhang, *J. Phys Chem. B*, 2004, **108**, 19510–19517.
- 35 S. Cha, M. Ao, W. Sung, B. Moon, B. Ahlström, P. Johansson, Y. Ouchi and D. Kim, *Phys. Chem. Chem. Phys.*, 2014, **16**, 9591–9601.
- 36 T. Shimomura, K. Fujii and T. Takamuku, *Phys. Chem. Chem. Phys.*, 2010, **12**, 12316–12324.
- 37 W. N. Martens, R. L. Frost, J. Kristof and J. T. Kloprogge, *J. Raman Spectrosc.*, 2002, **33**, 84–91.
- 38 K. Fujii, Y. Soejima, Y. Kyoshoin, S. Fukuda, R. Kanzaki, Y. Umebayashi, T. Yamaguchi, S. Ishiguro and T. Takamuku, *J. Phys. Chem. B*, 2008, **112**, 4329–4336.
- 39 A. Wulf, K. Fumino and R. Ludwig, *Angew. Chem. Int. Ed.*, 2010, **49**, 449–453.
- 40 I. Rey, P. Johansson, J. Lindgren, J. C. Lassègues, J. Grondin and L. Servant, *J. Phys. Chem. A*, 1998, **102**, 3249–3258
- 41 S. Tsuzuki, H. Tokuda, K. Hayamizu and M. Watanabe, *J. Phys. Chem. B*, 2005, **109**, 16474–16481.
- 42 R. Katoh, M. Hara and S. Tsuzuki, *J. Phys. Chem. B*, 2008, **112**, 15426–15430.
- 43 P. Nockemann, B. Thijs, S. Pittois, J. Thoen, C. Glorieux, K. Van Hecke, L. Van Meervelt, B. Kirchner and K. Binnemans, *J. Phys. Chem. B*, 2006, **110**, 20978–20992.
- 44 M. Yamagata, Y. Katayama and T. Miura, *J. Electrochem. Soc.*, 2006, **153**, E5–E9.
- 45 T. Takamuku, M. Tanaka, T. Sako, T. Shimomura, K. Fujii, R. Kanzaki and M. Takeuchi, *J. Phys. Chem. B*, 2010, **114**, 4252–4260.

- 46 T. Takamuku, T. Shimomura, M. Tachikawa and R. Kanzaki, *Phys. Chem. Chem. Phys.*, 2011, **13**, 11222–11232.
- 47 T. Takamuku, M. Tobiishi and H. Saito, *J. Solution Chem.*, 2011, **40**, 2046–2056.
- 48 T. Takamuku, H. Wada, C. Kawatoko, T. Shimomura, R. Kanzaki and M. Takeuchi, *Phys. Chem. Chem. Phys.*, 2012, **14**, 8335–8347.
- 49 K. Fujii, R. Kanzaki, T. Takamuku, T. Fujimori, Y. Umebayashi and S. Ishiguro, *J. Phys. Chem. B*, 2006, **110**, 8179–8183.
- 50 T. Takamuku, M. Tabata, M. Kumamoto, A. Yamaguchi, J. Nishimoto, H. Wakita and T. Yamaguchi, *J. Phys. Chem. B*, 1998, **102**, 8880–8888.

Figure Captions

Fig. 1 Structure of $C_2mimTFSI$ with the notation of the hydrogen, carbon, and nitrogen atoms within C_2mim cation.

Fig. 2 Raman spectra of the C–H stretching vibration band of the imidazolium ring of C_2mim cation in $C_2mimTFSI$ –DMSO solutions at various x_{DMSO} . The broken lines in the spectrum of pure ionic liquid ($x_{DMSO} = 0$) represent each component obtained by peak fits.

Fig. 3 Wavenumbers of the C–H stretching vibrations of the imidazolium ring of C_2mim cation in $C_2mimTFSI$ –molecular liquid solutions as a function of x_{ML} . Panels a and b represent the wavenumbers of the components at 3121 and 3170 cm^{-1} , respectively, for DMSO solutions determined from Raman spectra. Panels c and d indicate those of the components at 3125 and 3157 cm^{-1} , respectively, for DMSO, MeOH, and AN solutions determined from ATR-IR spectra.

Fig. 4 ATR-IR spectra of the C–H stretching vibration bands of the imidazolium ring of C_2mim cation in $C_2mimTFSI$ –molecular liquid solutions in the x_{ML} range from 0 to 1 at the intervals of 0.1 (left panels). Those of the in- and out-plane C–H bending vibrations of the ring in the same solutions (right panels). The upper (a and d), middle (b and e), and lower (c and f) panels represent the spectra of DMSO, MeOH, and AN solutions, respectively.

Fig. 5 1H and ^{13}C NMR spectra of $C_2mimTFSI$ –DMSO solutions at various x_{DMSO} in panels a and b, respectively.

Fig. 6 ^1H and ^{13}C NMR chemical shifts of the imidazolium ring in $\text{C}_2\text{mimTFSI}$ –molecular liquid solutions as a function of x_{ML} . The estimated standard deviations σ are indicated as error bars.

Fig. 7 ^1H and ^{13}C NMR chemical shifts of the ethyl and methyl groups of C_2mim cation in $\text{C}_2\text{mimTFSI}$ –molecular liquid solutions as a function of x_{ML} . The estimated standard deviations σ are indicated as error bars.

Fig. 8 ATR-IR spectra of the S=O stretching vibrations of DMSO in $\text{C}_2\text{mimTFSI}$ –DMSO solutions as a function of x_{DMSO} . Panels a, b, and c show the original spectra of the solutions at $x_{\text{DMSO}} = 0, 0.1, 0.2, 0.3, 0.4, 0.5, 0.6, 0.8, 0.85, 0.9, 0.95, 0.97, 0.99$, and 1, the difference spectra obtained by subtracting the spectrum of $\text{C}_2\text{mimTFSI}$ from the original spectra with taking into account the molarity of ionic liquid for the binary solutions, and the double difference spectra calculated by further subtraction of the spectrum of DMSO from the difference spectra, respectively.

Fig. 9 Plots of absorbance values of the negative peak at $\sim 1051\text{ cm}^{-1}$ and the positive peak at $\sim 1028\text{ cm}^{-1}$ in the double difference spectra of $\text{C}_2\text{mimTFSI}$ –DMSO solutions (Fig. 8c) against the x_{DMSO} .

Fig. 10 ATR-IR spectra of the asymmetric S=O stretching vibration bands of TFSI anion in $\text{C}_2\text{mimTFSI}$ –molecular liquid solutions over the x_{ML} range from 0 to 1 at the intervals of 0.1. Panels a, b, and c show the spectra of DMSO, MeOH, and AN solutions.

Fig. 11 Wavenumbers of the in-phase asymmetric S=O stretching vibration of TFSI anion in C₂mimTFSI–molecular liquid solutions as a function of x_{ML} .

Fig. 12 ¹³C NMR chemical shifts of the trifluoromethyl carbon atoms of TFSI anion in C₂mimTFSI–molecular liquid solutions as a function of x_{ML} . The estimated standard deviations σ are indicated as error bars.

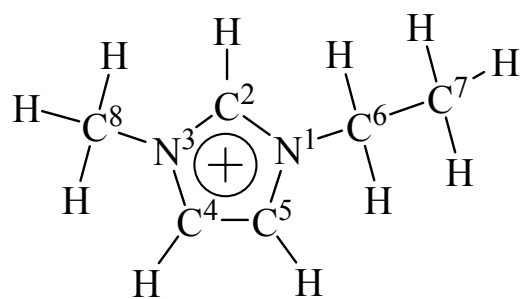


Fig. 1 T. Takamuku et al.

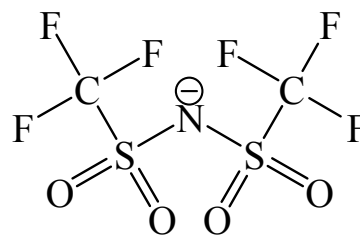


Fig. 2 T. Takamuku et al.

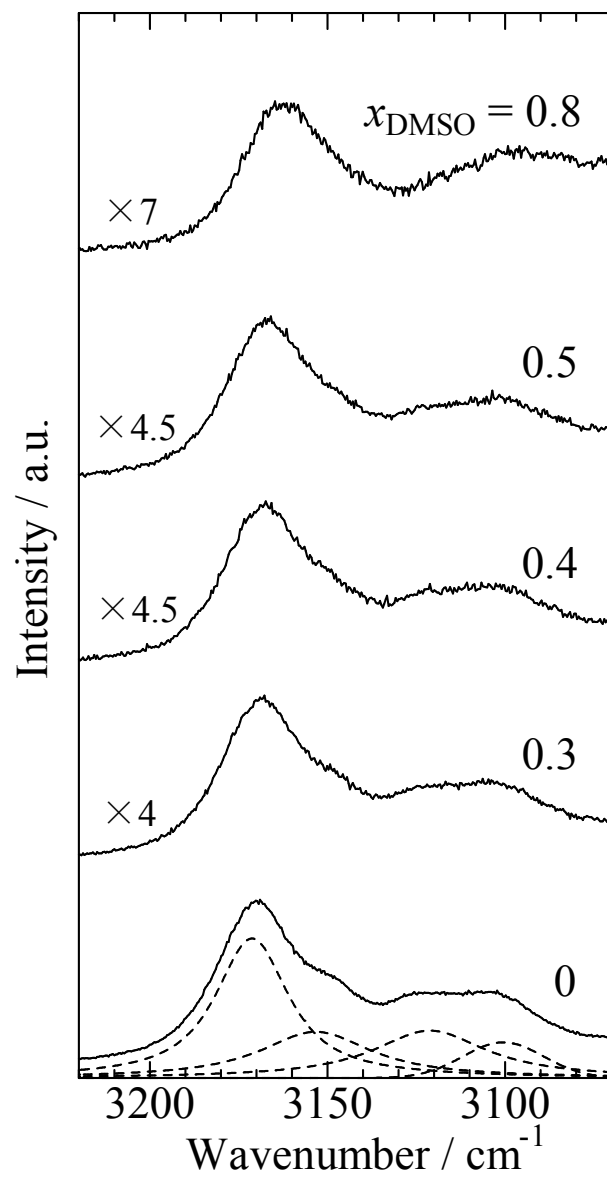


Fig. 3 T. Takamuku et al.

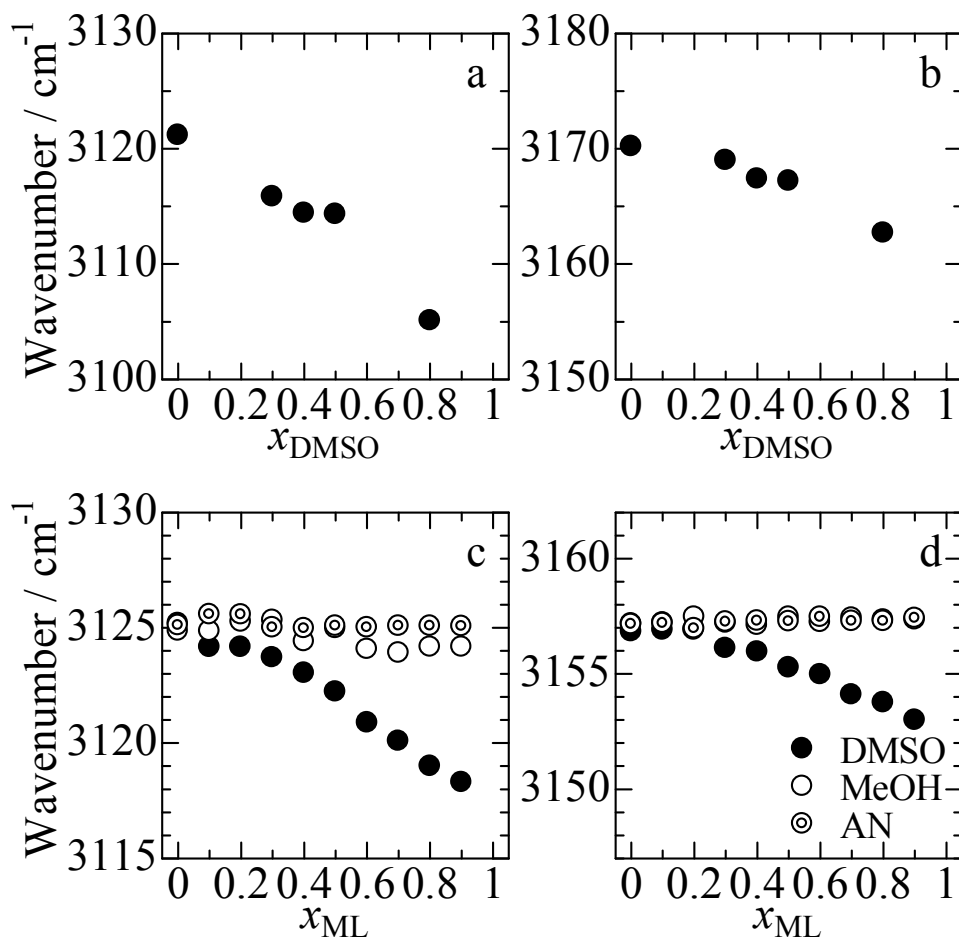


Fig. 4 T. Takamuku et al.

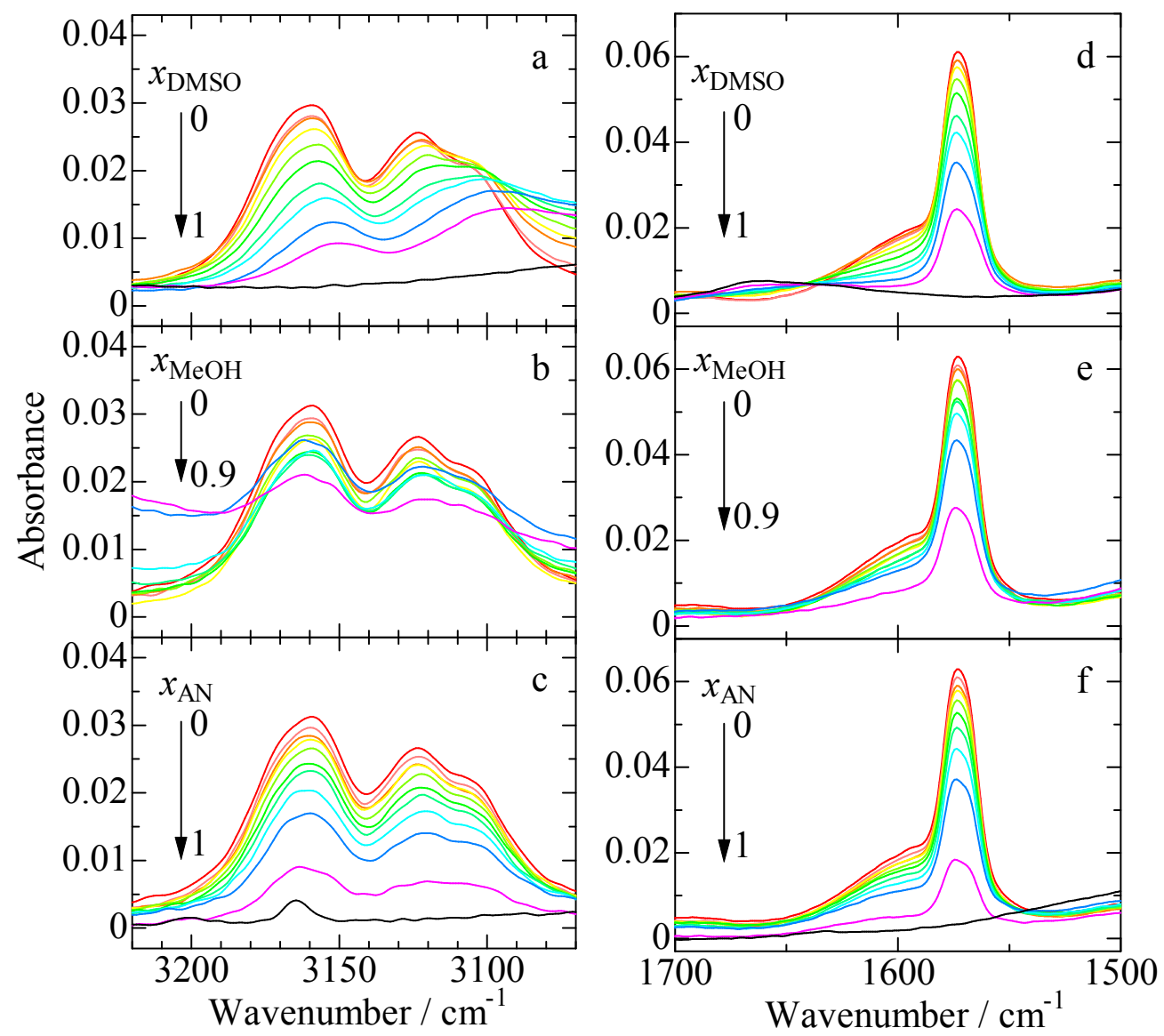


Fig. 5 T. Takamuku et al.

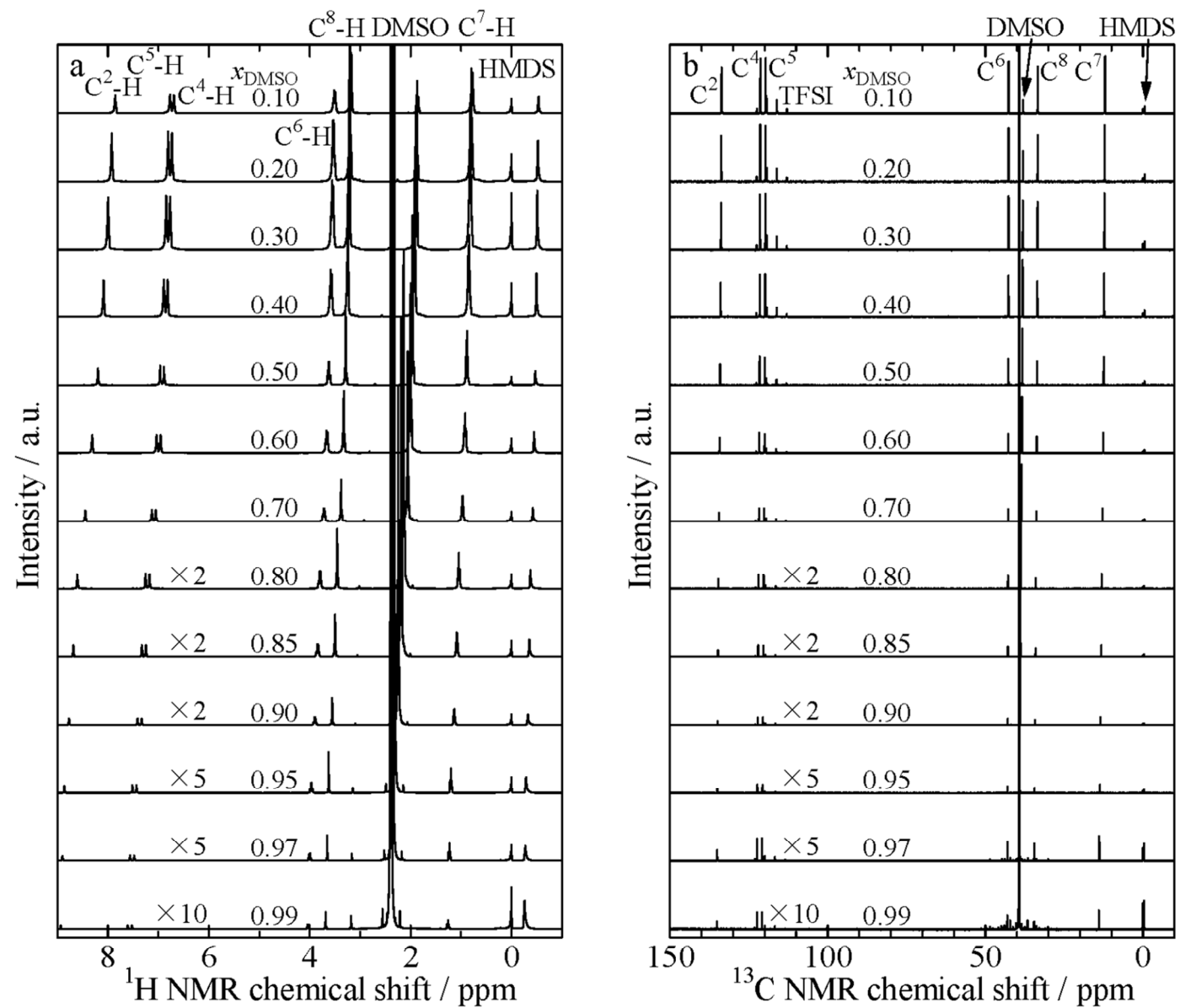


Fig. 6 T. Takamuku et al.

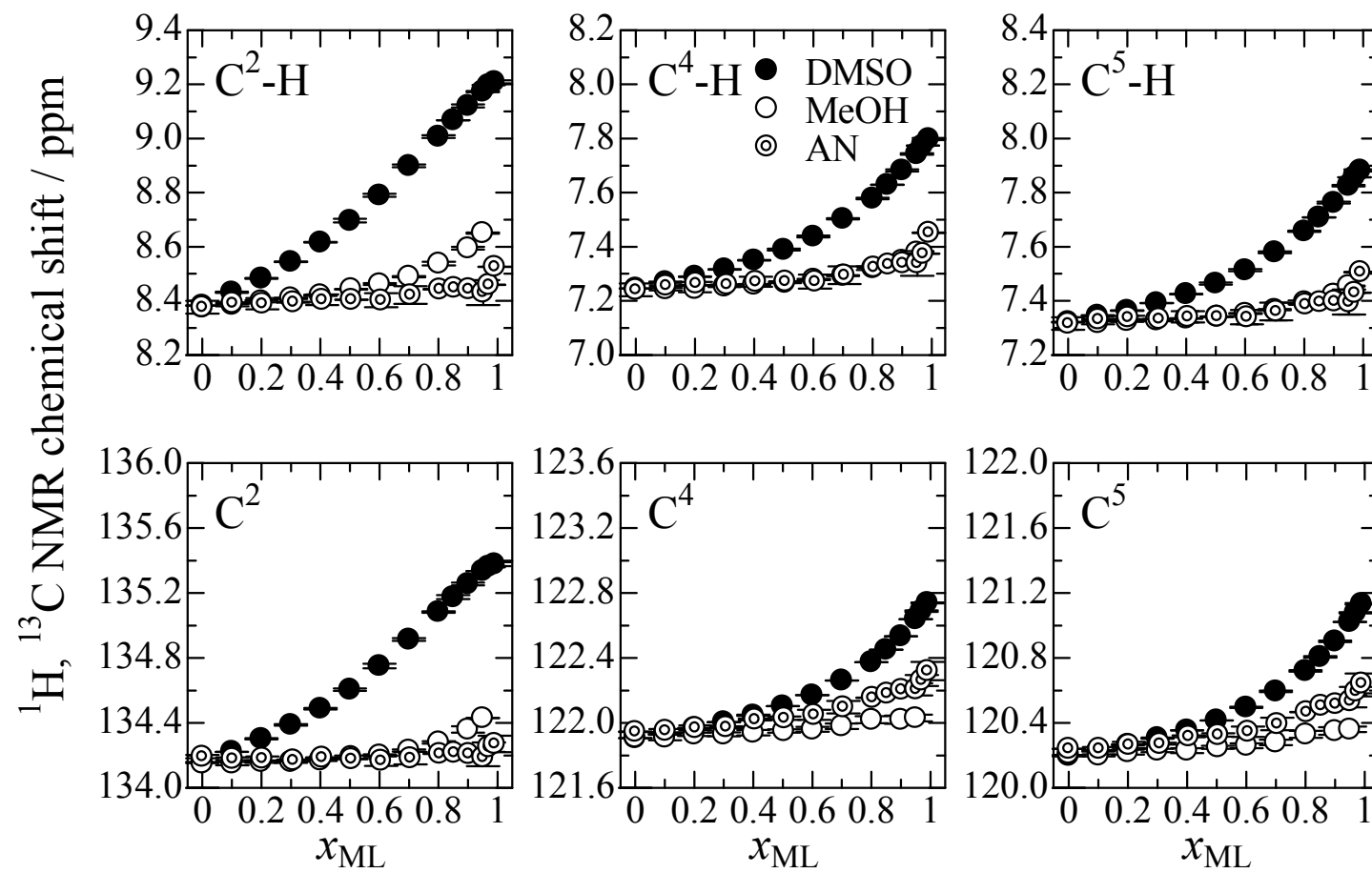


Fig. 7 T. Takamuku et al.

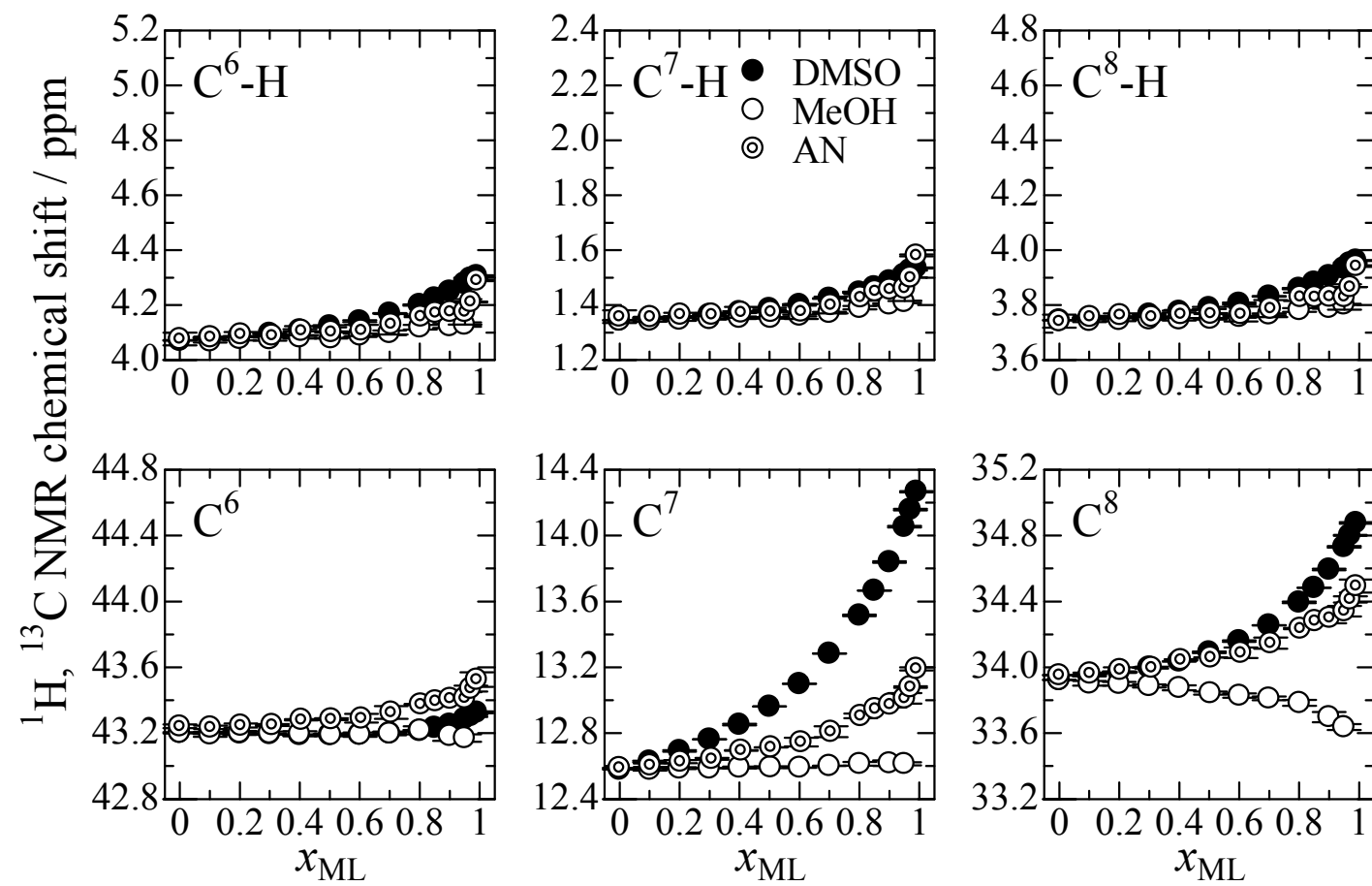


Fig. 8 T. Takamuku et al.

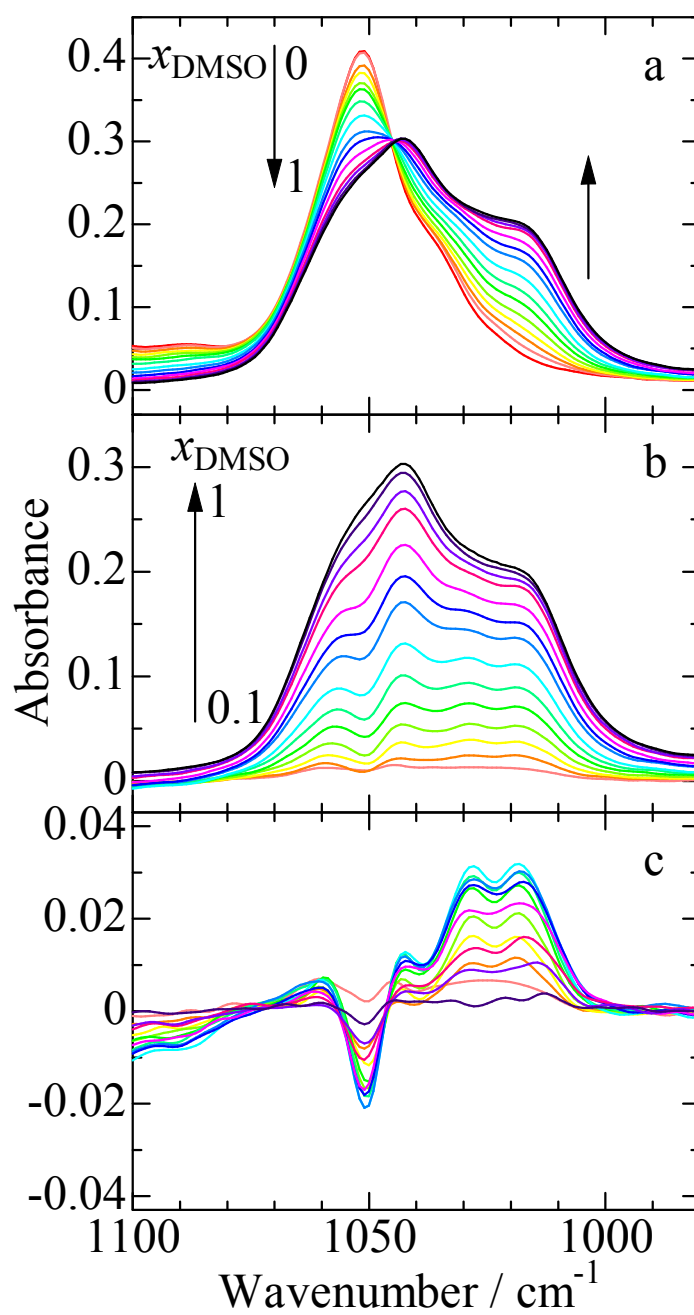


Fig. 9 T. Takamuku et al

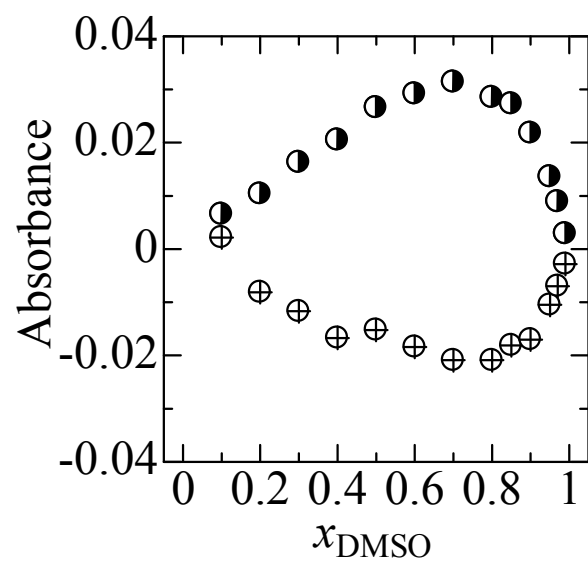


Fig. 10 T. Takamuku et al

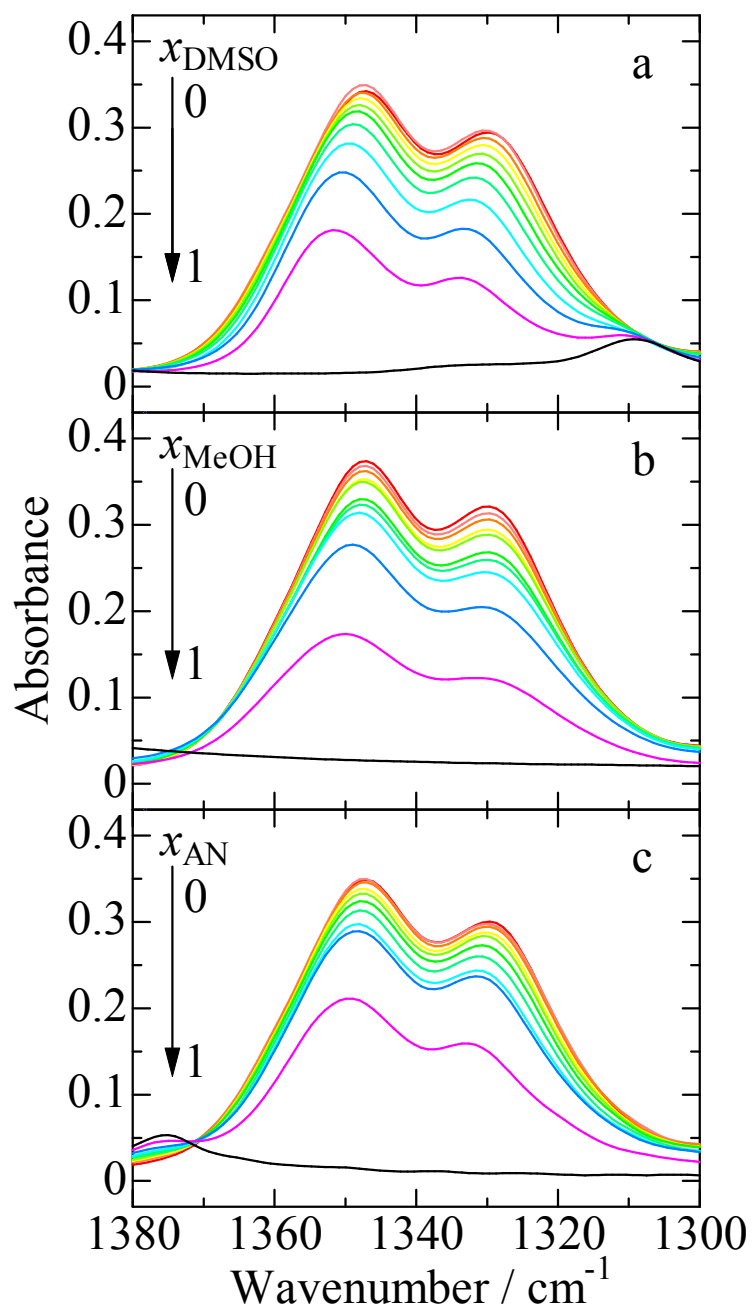


Fig. 11 T. Takamuku et al

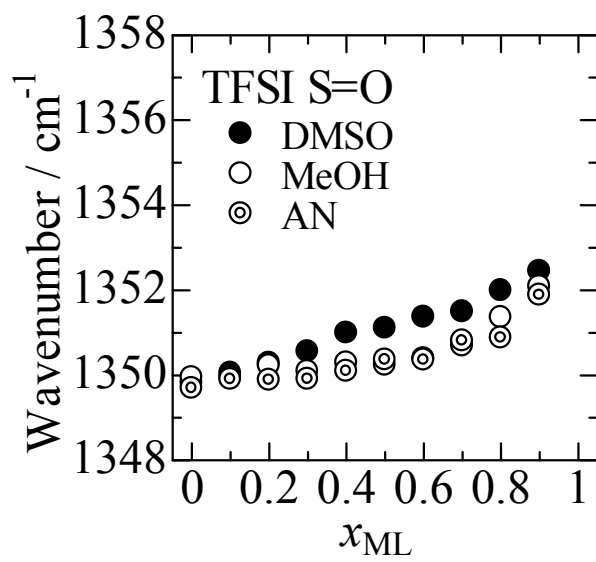
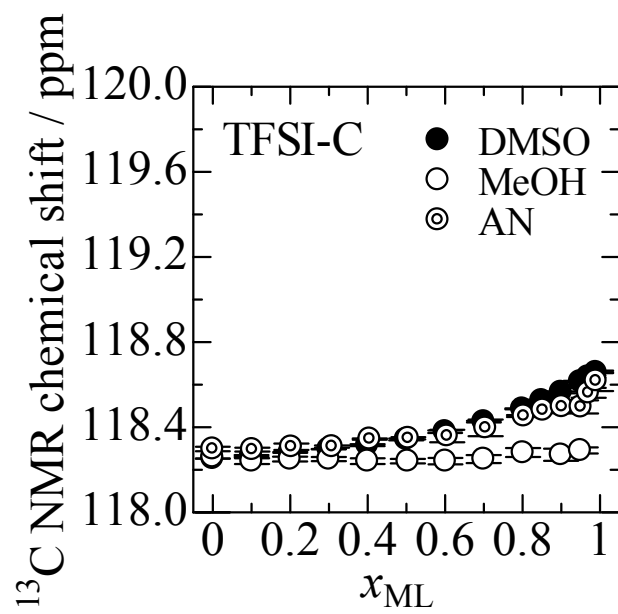
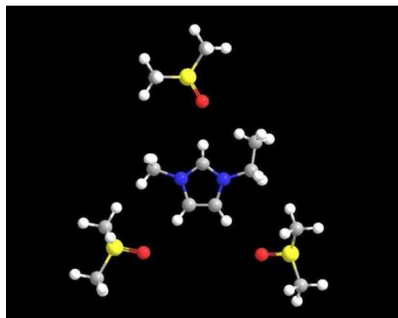


Fig. 12 T. Takamuku et al



Graphical Content T. Takamuku, et al



The hydrogen bonding between C₂mim cation and DMSO.